Contemporary Mathematics
Volume 119, 1991

Star-Shapedness of Digitized Planar Shapes

D. SHAKED, J. KOPLOWITZ, AND A. M. BRUCKSTEIN

ABSTRACT. We provide a definition of star-shapedness for digitized planar shapes, and an efficient tool for determining whether a given digitized planar shape is star-shaped or not. An equivalence is established, between the digital star-shapedness and the star-shapedness of the minimal perimeter polygon that separates object pixels from background pixels. The definition of digital star-shapedness presented here, is related to a class of definitions of digital shape features, such as the definitions of the digital straight line and the digital convexity.

1. Introduction

The *kernel* $K(S)$ of a planar shape S, is the set of points p of the shape S, such that for every point q of the shape boundary dS, the line segment $\overline{pq}$ lies entirely within the shape.

$$K(S) = \{p \in S \mid \forall q \in dS, \overline{pq} \subset S\}.$$

A planar object is said to be *star-shaped* if $K(S) \neq \varnothing$. We can view star-shapedness as an extension of convexity since, a shape is said to be convex if $K(S) = S$. Star-shapedness and the shape of the kernel are important for planar shape representation and analysis. The radial boundary representation of a planar object, for example, is possible only if the planar object is star-shaped and the radial origin lies in its kernel.

1.1. Previous results. Previous work in star-shapedness and the determination of the kernel of shapes, concerned only continuous shapes. Lee and Preparata introduced a linear, and thus optimal, algorithm for polygons [**LP**]. Based on this algorithm, Bornstein and Bruckstein provided an optimal algorithm for a general continuous shape, linear in the number of the boundary inflection points [**BB**].

1980 *Mathematics Subject Classification* (1985 *Revision*). Primary 52A30, 51M30, 52A43, 11H16.

This paper is in final form, and no version of it will be submitted for publication elsewhere.

This research was supported in part by the Technion V.P.R. Fund–Lowengart Research Fund.

0271-4132/91 $1.00 + $.25 per page

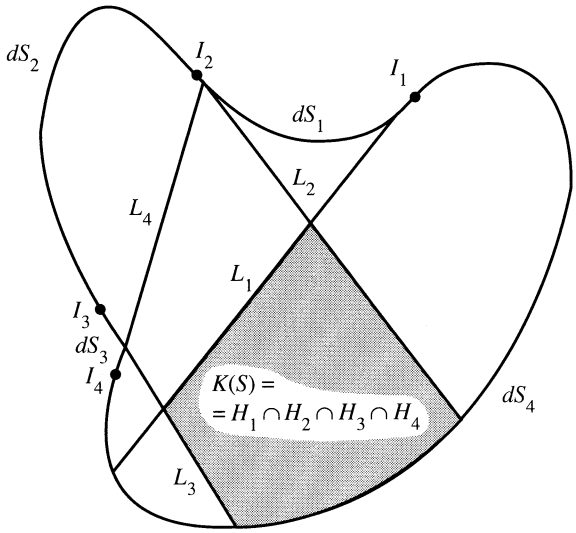

FIGURE 1. Continuous shape and kernel

Here we recall some of the results presented in **[BB]**, which will be used in the sequel. Let us partition the boundary dS of a shape S into disjoint portions $\{dS_1, dS_2, \ldots, dS_n\}$ called *boundary segments.* The partition points $\{I_1, I_2, \ldots, I_n\}$ include all the inflection points of dS, so that each segment dS_i is either concave or convex. Let us define now for every partition point I_i, a line L_i, the tangent of the shape at I_i. Using L_i we define the interior half-plane H_i, interior being defined by the inner side of dS at I_i.

In **[BB]** it was shown that the following procedure yields the kernel of the shape (see Figure 1). If the turn angle (turn angle is defined as the change of the segments tangent angle between the segments end points), of any boundary segment dS_i, is not in the interval $[-\pi, 3\pi]$ then $K(S) = \varnothing$, otherwise:

$$K(S) = \left[\bigcap_{i=1}^{n} H_i\right] \cap S.$$

It was also shown that if dS contains a boundary segment (not necessarily purely concave or convex) whose turn angle is not in the interval $[-\pi, 3\pi]$, then $K(S) = \varphi$. Bornstein and Bruckstein find the kernel using this simple representation of the kernel and an algorithm similar to Lee and Preparata's.

1.2. Motivation. Digital shapes are usually considered as planar objects made out of grid squares (pixels), that were obtained from a continuous shape by an imaging transformation or spatial sampling process (see next section). We would like the digitized shapes to preserve the features of the original shapes, in our case star-shapedness. If the original shape is star-shaped we would also like to preserve the shape of the kernel. It is easy to see that a straightforward extension of the continuous definitions to digitized

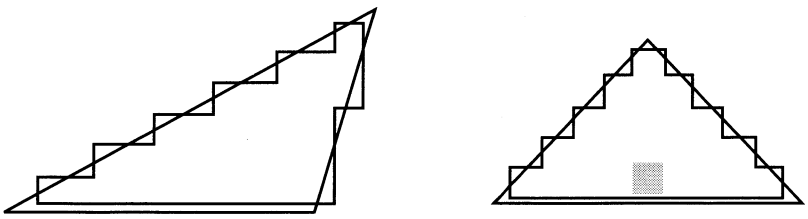

(a) Sampled triangle has no kernel. (b) Sampled triangle has a small kernel.

FIGURE 2. Two sampled triangles

shapes is worthless. In Figure 2 two triangular shapes and their corresponding digital shapes are shown. One can see that in one case the digital shape has no kernel, and in the other the kernel of the digital shape is a small part of the shape. Considering that all triangles are convex, and that for all convex shapes the kernel is the shape itself, it is obvious that the application of the usual definition to digital shapes is meaningless.

Fortunately, the star-shapedness is not the first digital feature suffering from this phenomenon. Straight lines and convex shapes raise similar problems in their digital equivalents. The definition proposed herein for digital star-shapedness is similar in spirit to the usual definitions of digital lines and digital convexity [**SCH, SK, KR**]. A digital line, or straight edge is a digital boundary that has a straight preimage. Similarly a digital convex shape is a digital shape for which a convex preimage exists. (A preimage is a continuous shape whose digitization is the given digital image). Our definition of the digital kernel and digital star-shapedness is analogous to the above definitions, though due to the special nature of the star-shapedness a few complications to the basic notion are unavoidable.

The resulting definition of the digital star-shapedness, like the simpler definitions of the digital line and digital convexity, is not applicational. The main purpose of this paper is to present an alternative definition equivalent to the proposed definition. In the following we introduce an equivalence between the digital star-shapedness and the star-shapedness of the minimal perimeter polygon that separates object pixels from background pixels. This result, together with existing algorithms for the extraction of minimal perimeter polygons, and the calculation of kernels in polygons, form an applicational alternative for the definition of digital kernel and digital star-shapedness.

In the next section, we introduce some definitions and symbols that we use. We conclude that section with the definition of the digital kernel and digital star-shapedness. The following section will be devoted to relating digital star-shapedness to the star-shapedness of the minimal perimeter polygon.

2. Definitions

2.1. Imaging. The digitization method we relate to is the square grid point sampling, in which a square planar grid is superimposed on an image, and the

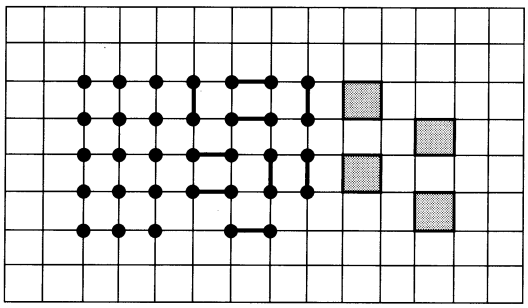

FIGURE 3. The three basic elements of the digital plan (shown on a grid): grid points, line segments, and units

grid points are labeled 1 or 0 according to whether they lie inside or outside the imaged shape. The case where a grid point lies exactly on the boundary of S, is ambiguous, and we assume the grid point is then labeled arbitrarily.

In the sequel a digital shape will be usually denoted DS. Sometimes, we will specify the digitization or imaging of the continuous shape S by $DS(S)$.

2.2. The digital plane. Since we relate to a rectangular imaging method, the usual neighborhood system in the grid points is defined. A digital shape is *4 connected* if every pair of grid points in the shape can be connected by a sequence of 4 neighbor points of the shape.

Let us define the basic elements of the digitized plane. We relate to three basic elements (see Figure 3).

(1) Grid points.
(2) Line segments connecting 4-neighbor grid points.
(3) Squares bounded by those line segments defined as *units.*

Note that the boundaries of the units are the line segments, and that the unit vertices are grid points. We define two kinds of units. A unit whose vertices are uniformly labeled grid points is a *Uniform unit*, otherwise it will be called a *Boundary unit.* Vertices of boundary units are *Boundary grid points.* Having defined the basic topological elements we can define the following regions of the digital plane, see Figure 4:
The *background region*:

$BACK(DS)$ = {The union of;
1. All grid points labeled 0,
2. All line segments between them,
3. All uniform units labeled 0}

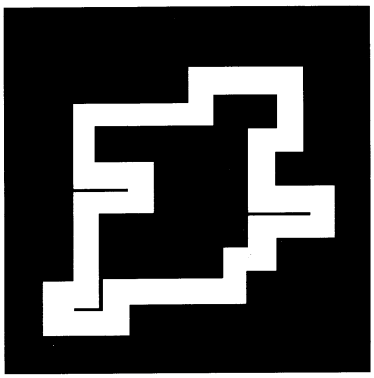

(a) A shape in the continuous plane R^2, with the sampling grid.

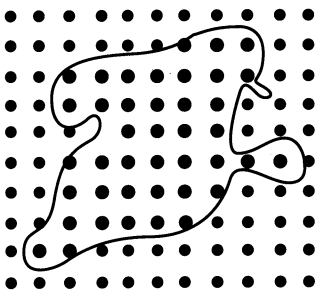

(b) The inner and outer dark shapes are the inner region $IN(DS)$, and the background region $BACK(DS)$ respectively. The region between them is the boundary zone dDS.

FIGURE 4. Shapes of the digital plane

The *inner region*:

$IN(DS) = \{$The union of:

1. All grid points labeled 1,
2. All line segments between them,
3. All uniform units labeled 1$\}$

If we consider how our intuition usually translates a digital image, we see that the two regions defined above are the areas we are quite sure of. The inner region is quite surely inside the shape we perceive in the digital plane, and the background region is quite surely in the background of the shape digitized. While practically, especially in cases of poor sampling, this interpretation may not always be a true interpretation of the digitized shape, those regions seem to be a good representation of the common sense interpretation of digitized images. As the sampling density improves this intuitive interpretation eventually becomes precise.

We will use these basic regions to define another region in the digital plane. The *boundary zone* dDS is a region containing all points we are not really sure of. It contains all points that are neither in $IN(DS)$ nor in $BACK(DS)$.

$$dDS = (IN(DS) \cup BACK(DS))^c,$$

where x^c represents the complementary of x in the plane.

See Figure 4 and note that $IN(DS) \cap BACK(DS) = \varnothing$, and that the boundary units that constitute the boundary zone dDS separate $IN(DS)$ from $BACK(DS)$.

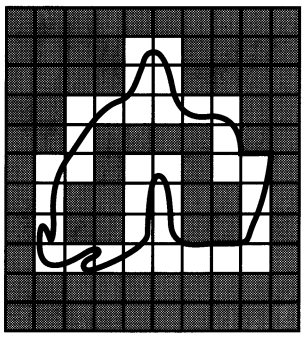

(a) A simple-preimage

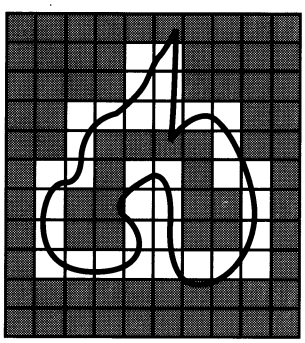

(b) The boundary of the preimage crosses the boundary of dDS, and therefore the shape is not a simple-preimage. Note that parts of the shape boundary are not in dDS.

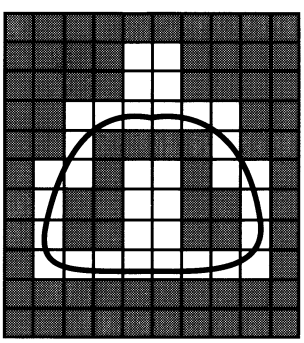

(c) The boundary dS of the shape in the figure is either in or on the boundary of dDS, but since dS crosses the boundary of dDS, S is not a simple-preimage.

FIGURE 6. A simple and two nonsimple preimages

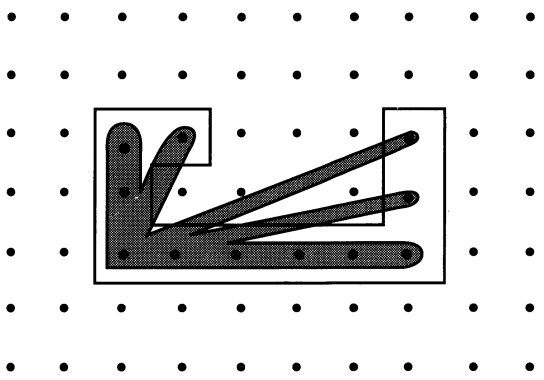

FIGURE 7. An example of a star-shaped preimage for a definitely non-star-shaped digital image

polygon is well defined, and is the relative convex-hull of $IN(DS)$ relative to $BACK(DS)$ [**SK**].

We define the *kernel* $K(DS)$ of a digital shape DS as the intersection between $IN(DS)$ and the union of the kernels of all the simple-preimages:

$$K(DS) = \left[\bigcup_{S \in SI(DS)} K(S) \right] \cap IN(DS).$$

A digital shape DS will be defined as *digitally star-shaped* if $K(DS) \neq \varnothing$. Note that if there exists a star-shaped simple-preimage S and $K(S) \cap IN(DS) \neq \varnothing$, then $K(DS) \neq \varnothing$ and DS is star-shaped. Note also that:

(1) Digital shapes that are not 4-connected with a 4-connected background have no kernel $(K(DS) = \varnothing)$.

(2) While the definitions of the digital line and the digital convexity are based on the existence of a proper preimage, our definition is based on the existence of a proper simple-preimage. Indeed the simple-inverse set $SI(DS)$ does not contain all preimages, but as it was demonstrated above, most of the preimages $SI(DS)$ excludes are odd shapes, that mislead the intuition and would usually be consequences of poor sampling. Such preimages may also disagree with our idea of what the digital star-shapedness should be. An extreme example of a definitely non-star-shaped digital image and its star-shaped preimage is shown in Figure 7. In the definitions of the digital straight line and digital convexity this limitation was not necessary, since those features have an inherent smoothness that readily precludes preimages not in $SI(DS)$.

(3) We limit the digital kernel to be part of $IN(DS)$. This limitation is due to the shape/background ambiguity of the boundary zone dDS. If we want our kernel to be definitely included in the shape, it has to be limited to $IN(DS)$.

3. Results

The definition of the digital kernel as presented above is clearly not applicable. The main result of this work is a "simplification" of the definition. In Theorem 1 we show that the kernel of a digital shape as defined above is the intersection of $IN(DS)$ and the kernel of the minimal perimeter polygon of the digital shape:

$$K(DS) = K(MPP(DS)) \cap IN(DS).$$

This result makes the proposed definitions of the digital kernel and digital star-shapedness practical.

To prove Theorem 1, we have to show that both

$$K(DS) \subset K(MPP(DS)) \cap IN(DS),$$

and

$$K(DS) \supset K(MPP(DS)) \cap IN(DS).$$

Recalling the definition of the digital kernel, it is clear that the second equation is trivially true, since $MPP(DS) in SI(DS)$. Using the same definition, the first equation becomes

$$K(S) \cap IN(DS) \subset K(MPP(DS)) \cap IN(DS), \quad \text{for } \forall S \in SI(DS).$$

In Theorem 0 we prove the last equation for all shapes in a subset of $SI(DS)$. Most readers will find the extension of the proof to $SI(DS)$ quite natural and obvious. The full proof of the last equation, and with it the conclusion of Theorem 1 is, however, given in the appendix.

Let us then focus on the subset $LSI(DS) \subset SI(DS)$. We call this set the *limited simple-inverse set.* Shapes in $LSI(DS)$ are called *limited shapes* or *limited simple-preimages.* Let dS and $dMPP$ be the boundaries of S and $MPP(DS)$ respectively. A limited shape $S \in SI(DS)$ conforms with 4 limitations, see Figure 8:

(1) The set of points $dS \cap dMPP(DS)$ does not contain boundary segments, only isolated points.
(2) The boundary dS crosses $dMPP(DS)$ at all intersection points, i.e., at any point $dS \cap dMPP(DS)$, dS and $dMPP(DS)$ switch sides.
(3) All intersection points are neither on $IN(DS)$ nor on $BACK(DS)$, i.e.,

$$(dS \cap dMPP(DS)) \cap (IN(DS) \cup BACK(DS)) = \varnothing.$$

(4) S does not have a vertex at an intersection point, therefore the tangent to S at any such point is well defined.

We rely on the following known properties of the relative convex-hull [**SK**]:

(1) All convex vertices of $MPP(DS)$ are on $IN(DS)$.
(2) All concave vertices of $MPP(DS)$ are on $BACK(DS)$.

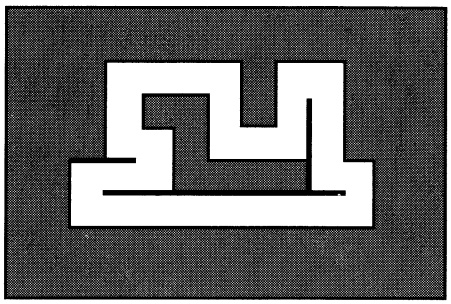

(a) A digitized shape DS represented by its inner and background regions $IN(DS)$ and $BACK(DS)$.

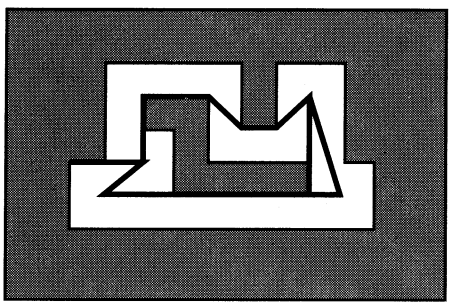

(b) The digitized shape DS and its minimal perimeter polygon $MPP(DS)$.

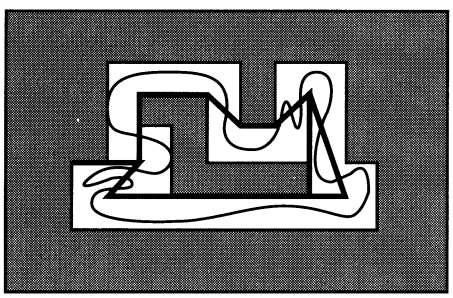

(c) A limited simple preimage, $S \in LSI(DS)$.

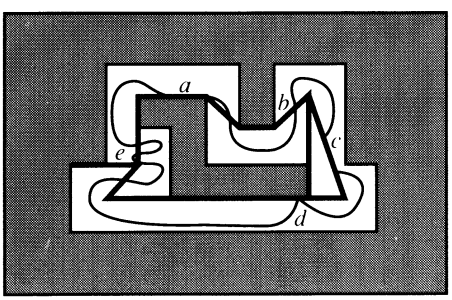

(d) A nonlimited simple preimage. Note the five details a–e, (the reasons why the shape is not limited). Details (a) does not satisfy limitation numbers 1 and 3, detail (b) limitation 4, detail (c) limitations 1 and 4, detail (d) limitations 2, 3, and 4, and detail (e) does not satisfy limitation number 2 (and there are many more combinations and variations).

FIGURE 8. Nice shapes

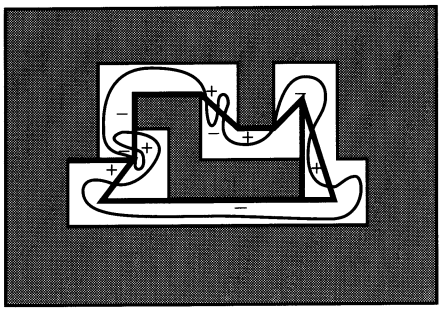

FIGURE 9. A labeling example. + indicates a concave labeling of the boundary segment $dMPP_i$, and − indicates a convex labeling of the segment.

For every shape in $LSI(DS)$, let us define a partition of $dMPP$ by a series of partition points $I = \{I_i\}$. The points of $dS \cap dMPP(DS)$, ordered on $dMPP(DS)$ are denoted $\{I_i\}$. Based on the above properties of the relative convex-hull and the definition of limited simple-preimages, we can show that the partition of $dMPP$ by the partition points series I has the following properties:

PROPERTY 1. This property classifies the boundary segments $dMPP_i$, that the partition $I = \{I_i\}$ defines on $dMPP(DS)$. We first note that all inflection edges of $dMPP$ have one vertex on $IN(DS)$ and another on $BACK(DS)$. As a result, the boundary of any limited shape $S \in SI(DS)$ crosses all inflection edges of $dMPP$ at least once. Therefore, for every limited simple-preimage, the partition $I = \{I_i\}$, is a partition for which the boundary segments $\{dMPP_i\}$ are purely concave or convex or straight lines (which are both concave and convex). Note that, on the contrary, in a general partition some boundary segments may include convex and concave vertices of $dMPP(DS)$ in the same boundary segment, such boundary segment would be neither concave nor convex.

PROPERTY 2. The boundary segments $dMPP_i$ of the partition I may be alternatingly labeled as concave or convex. We can demonstrate this property by suggesting the following labeling. Let us label all boundary segments $dMPP_i$ that are outside S, as concave boundary segments, and all segments $dMPP_i$ that are inside S, as convex segments. The suggested labeling has the desired property since dS and $dMPP(DS)$ cross at each partition point. What remains to be shown is that boundary segments $dMPP_i$ that contain a vertex are labeled by the suggested labeling according to their true nature. This, however, is obvious since all convex vertices of $MPP(DS)$ are on $IN(DS)$, and therefore all boundary segments $dMPP_i$ containing a convex vertex, have to be inside S. Similarly, all segments $dMPP_i$ containing a concave segment have to be outside S. See Figure 9.

REMARK 3a. This property is a trivial property concerning the relative

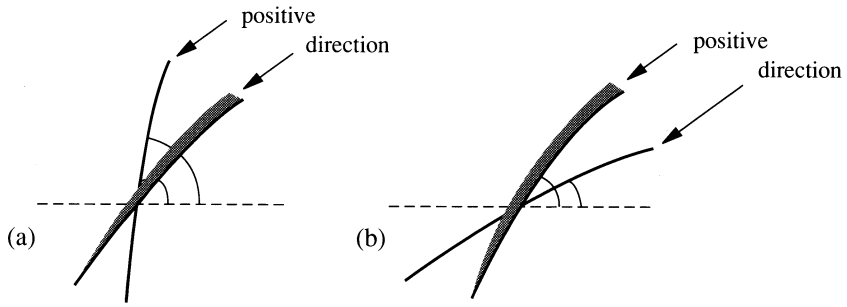

FIGURE 10. Following the positive direction, if the thin line "enters" the thick line, its angle is always bigger. If it exits, it exits with a smaller angle than the thick line has in that point.

size of the angles of dS and $dMPP$ at the partition points. For the sake of accuracy it should be mentioned, that by referring to "the angle of a curve at a point", we actually mean "the angle to the tangent to the curve at the point". Note that the tangent to both dS and $dMPP(DS)$, at the partition points $\{I_i\}$, is well defined.

At a point I_i of the partition, in which $dMPP$ turns from convex to concave, dS switches sides from outside to inside of $MPP(DS)$, consequently the angle of dS at I_i is larger then the angle of $dMPP$ at I_i. Similarly, at a point I_i in which $dMPP$ turns from concave to convex, dS exits $dMPP$, and its angle is smaller then the angle of $dMPP$ at I_i, see Figure 10.

PROPERTY 3b. An immediate result of Property 3a, compares the turn angle of the boundary segment $dMPP_i$, to the turn angle of the boundary segment dS_i (a segment of dS bounded by the same partition points as $DMPP_i$). We recall that the turn angle of a boundary segment is the angle of the boundary at the end of the segment minus the angle of the boundary at the beginning of the segment.

If $dMPP_i$ is convex, it has a smaller turn angle then dS_i, and if $dMPP_i$ is concave, it has a larger turn angle then dS_i. (Since in concave segments both turn angles are negative, the turn angle of $dMPP_i$ is, like in convex segments, smaller in absolute value).

Using those properties, we can prove Theorem 0.

THEOREM 0.

$$K(S) \cap IN(DS) \subset K(MPP(DS)) \cap IN(DS), \quad \textit{for } \forall S \in LSI(DS).$$

PROOF. Consider, an arbitrary limited simple-preimage. Find the ordered set of points $dS \cap dMPP$, and denote it $I = \{I_i\}$. Denote the half plane defined by the inner side of the tangent to $dMPP$ at I_i, by Hp_i. Note that I is the partition referred to in Properties 1-3b. Since Property 1 assures us that $\{dMPP_i\}$ are either concave or convex boundary segments, we can use

to

$$Hs_i \cap Hs_{i+1} \cap H_i^g \subset Hp_i \cap Hp_{i+1} \cap H_i^g .$$

We conclude our argument by claiming that from Property 3a it is obvious that both

$$Hs_i \cap H_i^g \subset Hp_i \cap H_i^g ,$$

and

$$Hs_{i+1} \cap H_i^g \subset Hp_{i+1} \cap H_i^g . \quad \text{Q.E.D.}$$

Note that Theorem 0 referred to all shapes in $LSI(DS)$. In the appendix we use Theorem 0 and extend it to all shapes in $SI(DS)$, thereby concluding the proof of Theorem 1.

3.1. Application. The original definition of the digital kernel, does not lead to any plausible algorithm for determining the digital kernel, nor to an algorithm determining whether the image is digitally star-shaped or not. The alternative definition, based on Theorem 1, has a straightforward implementation combining an algorithm determining the relative convex-hull [**T**], and an algorithm determining the kernel of a polygon [**BB**].

4. Summary

We have given a definition for star-shapedness of digitized planar shapes, in the spirit of the previous definition of digital convexity. It was shown that the kernel of a digital shape is the intersection of the inner region and the kernel of the minimal perimeter polygon of the digital shape, making the task of determining star-shapedness achievable. It should be noted that no use has been made of the assumption that the sampling method is a rectangular method. A generalization of the results for a nonsquare point-sampling method is quite immediate, and only involves a redefinition of 4 and 8 neighbors (a strong and weak neighbors in the general case).

Appendix

In the appendix the proof of Theorem 1 is finished. The proof of Theorem 0, referring to limited simple-preimages is extended gradually to apply to arbitrary simple-preimages. In each step a new set of shapes is introduced by lifting a part of the limitations on what we called limited shapes. Consequently the extended set of shapes is identical to $SI(DS)$, and Theorem 1 is proven.

Since the proof for every new set of shapes, is very similar to the proof of Theorem 0, we refrain from repetition, and denote only the changes that have to be made to include the new set of shapes in the proof. The main argument in the following proof, is the existence of a partition (not necessarily the partition $dS \cap dMPP(DS)$ of above), for which Properties 1–3b apply. Notice that once such a partition has been found for a certain simple-preimage, the proof of Theorem 0 applies for that shape as well.

THEOREM 1. $K(DS) = K(MPP(DS)) \cap IN(DS)$.

PROOF. The beginning of the proof is found in the top of §3. All that remains to be shown is that

$$K(S) \cap IN(DS) \subset K(MPP(DS)) \cap IN(DS),$$

for all shapes $S \in SI(DS)$, and not only in $LSI(DS)$ as was shown in Theorem 0.

(1) We first lift the last limitation that we used, and extend the proof to simple shapes that may have been considered as limited shapes if they had not had a vertex at a crossing point (see detail b in Figure 8d). This change necessitates only a semantic change in the partition. Since at the intersection point dS may not have a well defined tangent, we will choose an infinitesimally close point on dS as a partition point. We may choose an arbitrary side of the crossing point and use the limit point on dS from that side, as a partition point. The limit point is a proper partition point of $dMPP$, since dS is continuous, and the limit point is actually the crossing point itself, though now the tangent to dS at the point is well defined.

Note that, having cleared this semantic problem, the partition $I = \{I_i\}$ of ordered points in $dS \cap dMPP(DS)$ is a partition for which Properties 1–3b apply. The proof of Theorem 0 is therefore valid for the new set of shapes as well.

(2) Now we lift the second limitation, namely, shapes may also be "tangent" to $MPP(DS)$ (see detail e Figure 8d). In this case it can be easily shown that the partition which consists of all points $dS \cap dMPP(DS)$, except the tangension points, is a partition for which the properties are valid. Note that all four properties refer only to partition points in which dS actually crosses $dMPP(DS)$, an omission of the tangension points would therefore leave the properties valid.

(3) We next lift the first limitation. Here we consider simple-preimages whose boundary coincides with $dMPP(DS)$ on a boundary segment, not merely on isolated points. We keep though the remaining limitation, namely, none of the coincidence points may be on either $IN(DS)$ or $BACK(DS)$. Note that this implies that all the boundary *segments* in $dS \cap dMPP(DS)$, which from now on will be referred to as *coincidence boundary segments*, are straight line segments inside the boundary zone (see Figures 12(a–b) for shapes introduced in this stage and Figures 13–15 for shapes that are not introduced here).

For the new set of shapes, the set $dS \cap dMPP$ is uncountably large. From points in that set we select the following partition points. We take all isolated points in $dS \cap dMPP$, plus all the endpoints of the boundary segments in $dS \cap dMPP$.

It is easy to see that this partition agrees with Property 1. As for Property 2, since dS and $dMPP(DS)$ do not necessarily switch sides at all partition

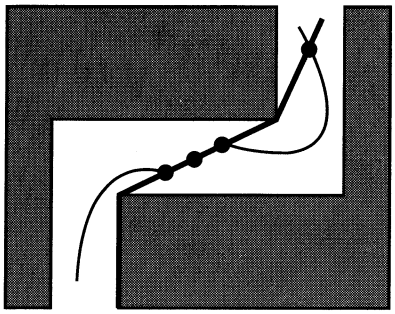

(a) A shape accepted in step 3, an extra partition point is needed in this case to maintain the alternating labeling of the boundary segments concave or convex.

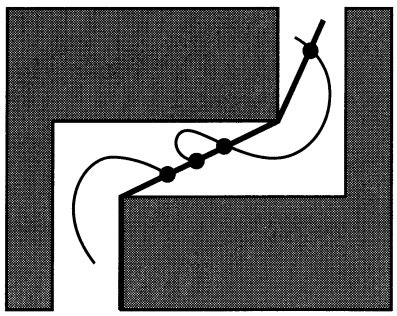

(b) A shape accepted in stage 3, no extra partition point needed to maintain alternating labeling.

FIGURE 12. Shapes accepted in step 3

points, we may have to add an additional partition point inside every coincidence boundary segment, so that the new partition will agree with Property 2. Note that we add the extra partition point, only in those coincidence boundary segments, where an additional boundary segment $dMPP_i$ is needed to maintain the alternating labeling of $\{dMPP_i\}$, (see Figure 12(a)). To conclude the adjustment to the properties, we also have to semantically modify Properties 2–3b:

> Instead of "inside/outside" in Property 2 we have to add "inside/outside or on the boundary of."
> Instead of "smaller/larger" in Properties 3a and 3b we have to add "smaller/larger or equal to."

(4) In this step we relieve a part of the last limitation that still remains. We accept in this step shapes whose coincidence boundary segment may be on either $IN(DS)$ or $BACK(DS)$ as long as none of the partition points of step 3 (crossing points or coincidence boundary segment endpoints), is on either $IN(DS)$ or $BACK(DS)$ (see Figure 13). This step introduces a set of shapes whose boundary coincides with $dMPP$ for a long boundary segment. Also the shape $MPP(DS)$ itself is introduced in this stage. Thus, to satisfy Property 1, we have to consider some more partition points inside the coincidence boundary segments. We therefore add to the partition points a point in each of the inflection edges of $dMPP(DS)$, possibly included in a coincidence boundary segment.

(5) We now lift another part of the last limitation. We accept shapes that coincide with $IN(DS)$ or $BACK(DS)$ on a partition point, as long as the partition point is a coincidence boundary segment endpoint, (see Figure 14 on page 156). The limitation stands now only for those shapes whose boundary

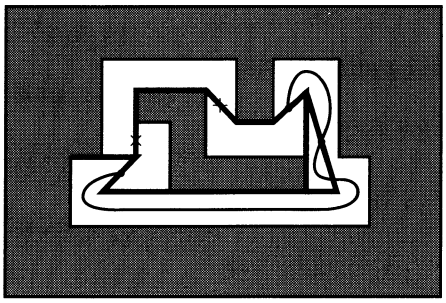

FIGURE 13. A shape accepted in step 4. The usual partition points are marked with dots; the partition prints added to them are marked by x.

is on $IN(DS)$ or $BACK(DS)$ in an isolated point of the set $dS \cap dMPP$, (see Figure 15 on page 157).

We separate all the shapes we have introduced in this stage according to the relative position of dS and $dMPP$ near the coincidence boundary segment endpoint. The following separation rule is very confusing, but once the duality of the inner and background regions is noticed, the separation rule may become clearer. (Note also that because of the duality Figures 12, 14, and 15 do not indicate the inner or background regions. Interpretation of the location of the shape-inside and the nature of the vertices (concave or convex) is possible in the two dual ways.)

If the coincidence segment is on $BACK(DS)$ and dS is inside $MPP(DS)$, or dually if the coincidence segment is on $IN(DS)$ and dS is outside of $MPP(DS)$, then we simply ignore that endpoint of coincidence segment. The reason we can do that is that dS in that case is on the right side of $dMPP$ (outside if $dMPP$ is convex and inside if $dMPP$ is concave), see Figure 14(a–b) on page 156.

If on the other hand, dS is on the wrong side of $dMPP$ (outside if the coincidence segment is on $BACK(DS)$ or inside if the coincidence segment is on $IN(DS)$), then the coincidence segment endpoint may be the only point in which dS coincides with a certain inflection edge, and we would certainly have to keep it, as a partition point, (see Figure 14c). The problem that arises while taking this kind of points as partition points is, that $dMPP$ may, and indeed would usually have a vertex at those points. The semantic problem that arises is easily solved in a way similar to the case of vertices on dS, at step 1. What we formally do, is to define the partition point as the limit of points *not* in the coincidence segment. It should be noted that to satisfy Property 1, the partition point should be a point on the inflection edge, and therefore a limit point from the outside of the coincidence boundary segment. A special note should be made in this case, concerning the possibility, that also dS may not have a well defined tangent at the same point. The partition point on dS could not (as in step 1) be the limit point

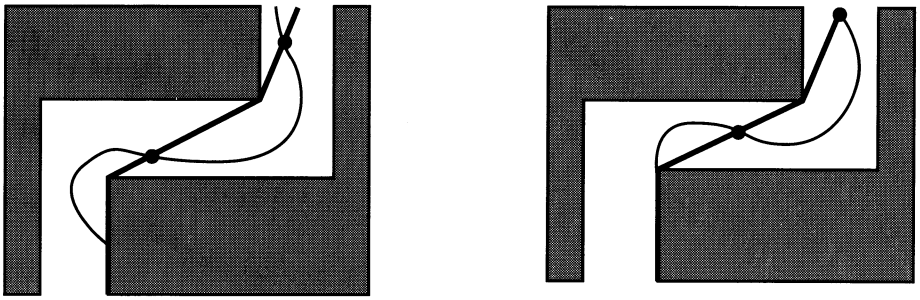

(a), (b) The boundary dS leaves $dMPP$ to the "correct" direction and therefore the possible partition at the coincidence boundary segment end-point is not being used. (Note that because of the IN/BACK duality we do not define either IN/BACK or inside/outside or concave/convex in the figure).

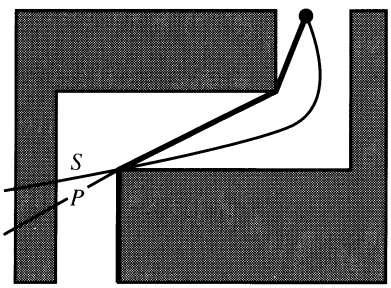

(c) The boundary dS leaves $dMPP$ to the "wrong" direction, and the coincidence boundary segment end-point is being taken as a partition point. (One might interpret those shapes as shapes in which dS crosses an inflection edge of $dMPP$ at the coincidence boundary segment end-point. The tangents of the shape and polygon are denoted s and p respectively.

FIGURE 14. Shapes accepted in step 5

from an arbitrary direction. To satisfy Properties 3a–b the direction, in this case, should correspond to the direction of the limit point on $dMPP(DS)$, namely, outside of the coincidence boundary segment.

Taking those precautions the partition agrees with Properties 1–3b, and the proof is valid for such shapes as well.

(6) At this last step we lift the last limitation on shapes, by accepting also shapes that may be on either $IN(DS)$ or $BACK(DS)$ also at isolated coincidence points, see Figure 15. To do that consider the coincidence point I_i as if it were an infinitesimally small coincidence boundary segment with two endpoints, a limit point from each side. If from the criteria of step 5 we would not have taken any of the endpoints as a partition point, we do not

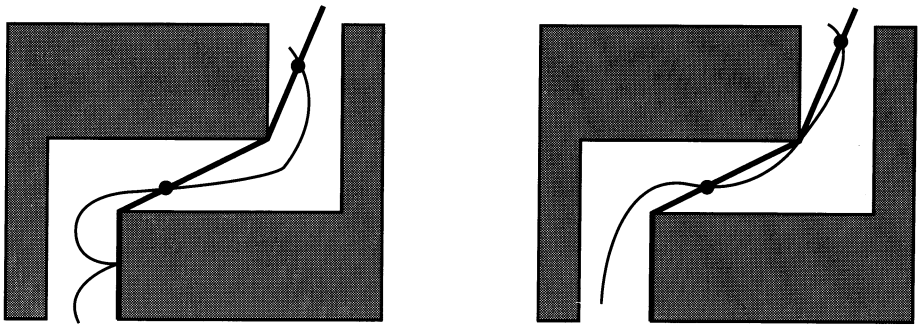

(a), (b) No partition point is needed in those cases.

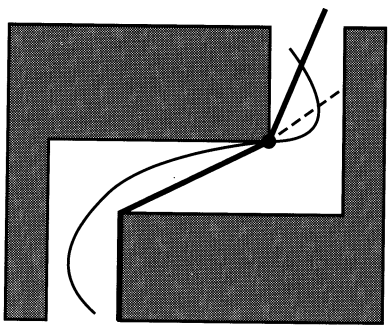

(c) A single partition point

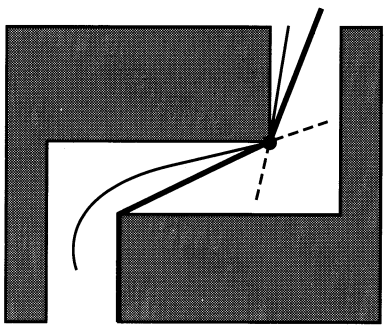

(d) Two partition points, each with a different tangent, are assigned to the same coincidence point, creating an infinitesimally small boundary segment.

FIGURE 15. Shapes accepted in step 6. The partition points are marked by dots and tangents by a broken line

take I_i as a partition point. If on the other hand we would have taken only one endpoint as a partition point, we will take I_i as a partition point, and define the angles of dS and $dMPP$ at that point exactly as we would have defined them for the segment endpoint we would have taken. The interesting case is, however, when from the criteria of step 5 it appears that we would have taken both endpoints of the coincidence segment, in this case we have to let I_i appear twice in the partition point series, which implies that we regard the coincidence point I_i as a boundary segment $dMPP_i$ with a turn angle equivalent to the angle of the vertex of $dMPP(DS)$ at I_i (simultaneously we regard I_i also as a boundary segment dS_i with a turn angle equivalent to the turn angle of the vertex dS has on I_i).

Since in this stage the set of shapes for which the equation is proved is $SI(DS)$, this concludes the proof of Theorem 1. Q.E.D.

REFERENCES

[BB] R. Bornstein and A. Bruckstein, *Finding the kernel of planar shapes*, EE Pub., No. 694, Technion Haifa, Israel, Dec. 1988.

[T] G. Toussaint, *An optimal algorithm for computing the relative convex-hull of a set of points in a polygon*, EURASIP 1986, pp. 853–856.

[LP] D. T. Lee and F. P. Preparata, *An optimal algorithm for finding the kernel of a polygon*, J. ACM **26** (1979), 415–421.

[SCH] J. Sklansky, R. L. Chazin, and B. J. Hansen, *Minimum perimeter polygons of digitized silhouettes*, IEEE Trans. Comp. **C-21** (1972), 260–268.

[SK] J. Sklansky and D. F. Kibler, *A theory of nonuniformly digitized binary pictures*, IEEE Trans. Systems Man Cybernet. **SCM-6** (1976), 637–647.

[KR] C. E. Kim and A. Rosenfeld, *Digital straight lines and convexity of digital regions*, IEEE Trans. PAMI, **PAMI-4** (1982), 149–153.

DEPARTMENT OF ELECTRICAL ENGINEERING, TECHNION—ISRAEL INSTITUTE OF TECHNOLOGY, HAIFA 32000, ISRAEL

DEPARTMENT OF ELECTRICAL AND COMPUTER ENGINEERING, CLARKSON UNIVERSITY, POTSDAM, NEW YORK 13676

DEPARTMENT OF COMPUTER SCIENCE, TECHNION—ISRAEL INSTITUTE OF TECHNOLOGY, HAIFA 32000, ISRAEL